Performance of Collimators Used for Tomographic Imaging of I-123 Contaminated with I-124

Joseph F. Polak, Robert J. English, and B. Leonard Holman

Harvard Medical School and Brigham and Women's Hospital, Boston, Massachusetts

Iodine-123 prepared from the $^{124}Te(p,2n)^{123}I$ reaction is contaminated with between 3% to 5% I-124 when imaging is performed. The effects of such a mixture were evaluated for medium-energy and low energy general-purpose collimators on a commercially available rotating gamma camera equipped to perform tomography. The planar sensitivity for I-123 was less for the general-purpose collimator, varying between 0.84 and 0.85 in water relative to that measured for the medium energy-collimator. Counts due to scattering or septal penetration of I-124 photons were greater for the general-purpose collimator (36%) than for the medium-energy collimator (15%). Evaluation of the higher-frequency components of the modulation transfer functions confirmed that the low-energy general-purpose collimator is expected to offer significantly more contrast information at frequencies above 0.21 cycles/cm. This is expected to contribute to image quality when studies are performed with collimators of similar design.

J Nucl Med 24: 1065–1069, 1983

I-123 produced by the $^{124}Te(p,2n)^{123}I$ reaction is less expensive and requires a less energetic proton beam than I-123 produced by the *p*,5*n* reaction. An undesired by-product of the *p*,2*n* reaction is the presence of small amounts of I-124 ($T_{1/2}$ = 4.2 days) whose decay produces enough high-energy photons to compromise seriously image quality due to scattered photons and to septal penetration in the collimator (*1–3*).

In order to assess the implications of using such contaminated I-123, we have evaluated the performance of a low-energy general-purpose and of a medium-energy collimator mounted on a rotating gamma camera (3/8-inch crystal) equipped to perform tomography. Both collimators were manufactured by casting and were 41 mm thick.

MATERIALS AND METHODS

Radionuclides. All I-123 imaging experiments were performed with less than 5% I-124 contamination. Estimates of the I-124 contribution to the original images were derived from measurements performed on Day 7, a time when the I-123 had decayed to insignificant levels.

Equipment and phantoms. A rotating gamma camera interfaced to a minicomputer was used to acquire and analyze the data.

Received Mar. 29, 1983; revision accepted May 19, 1983.

For reprints contact: B. Leonard Holman, MD, Dept. of Radiology, Harvard Medical School, 25 Shattuck St., Boston, MA 02115.

(1) *Planar images.* Digitized images of polyethylene (1 mm i.d.) line sources filled with a I-123/I-124 mixture were acquired in a 128-by 128-matrix format with a sampling interval of 0.24 cm/pixel.

(2) *Tomographic imaging.* The images were acquired with the frame digitization set to the 64-by 64-matrix format, with 64 regularly spaced angular increments. Acquisition times were set at 30 sec per angular projection.

The two collimators studied were: (a) a medium-energy collimator with 6000 hexagonal holes, 3.4 mm wide and 41.5 mm long, with septa 1.4 mm thick; and (b) a low-energy, general-purpose collimator with 18,000 hexagonal holes measuring 2.5 mm wide and 41 mm long, with 0.3-mm septa.

Line sources made of polyethylene with an internal diameter of 1 mm were imaged in air or at the center of a cylindrical phantom (20 cm diam) filled with water. Source distances were measured between the collimator face and the line source.

A cylindrical phantom 20 cm in diameter was also loaded with background activity of 0.3 μCi/ml and with cylindrical higher-activity targets 2.4 cm in diameter. The highest target-to-background ratio was set at 30:1, and others, in decreasing order, 15:1, 6:1, and 3:1.

Line spread functions. For both collimators, the line spread functions were measured at distances of 1, 5, 11, 16, 21, 31, and 36 cm from the collimator in air, and 11, 16, 21, 31, 36 cm from the center of the water-filled phantom. The FWHM was calculated after fitting a second-order polynomial to the three largest counts in a profile through the line source in order to find the maximum

and then interpolating between the points nearest half this value on each side of the curve. In each case, measurements were taken from ten different profiles through the line sources and then averaged.

Modulation transfer functions (MTFs). The line spread functions obtained on Day 1 and Day 7 (both sets made with a 159 keV window) were also used to calculate modulation transfer functions. The images taken on Day 7 resulted mostly from a broad 200 keV backscatter peak.

The calculation was performed on the line spread data L(i) according to the following formula (5):

$$MTF(r) = \frac{\left[\left(\sum_{i=-a}^{+a} [L(i) \cdot \cos(2\pi \cdot r \cdot i)]\right)^2 + \left(\sum_{i=-a}^{+a} [L(i) \cdot \sin(2\pi \cdot r \cdot i)]\right)^2\right]^{1/2}}{\sum_{i=-a}^{+a} L(i)}$$

where r = frequency in cycle/pixel and i = pixel number centered on the maximum of the line spread function.

Sensitivity and contribution due to I-124. Estimates of the counts contributed by I-124 were derived from the measured sensitivity on Day 7, when virtually no I-123 was detected, and then back-corrected for I-124 decay to the imaging times on Day 1. This contribution could then be subtracted from the total measured sensitivity, thus yielding the relative sensitivity to I-123 for both collimators. Contributions of scatter and septal penetration due to some of the higher-energy photons of I-123 are neglected so that the scatter fraction can be estimated to be due solely to I-124.

RESULTS

Full-width half-maximum (FWHM) determinations. The FWHM values are consistently less for the low-energy general-purpose collimator than for the medium-energy collimator (Fig. 1). At 11 cm, the FWHM values of the general-purpose collimator are 1.1 ± 0.03 and 1.2 ± 0.1 cm in air and water, respectively, compared with medium-energy values of 1.35 ± 0.03 and 1.45 ± 0.1 cm. At 21 cm the differences become more substantial, the values being 1.7 ± 0.09 and 1.88 ± 0.16 cm for the general-purpose collimator, against 2.08 ± 0.15 and 2.29 ± 0.21 cm for the medium-energy collimator.

Determinations of modulation transfer function (MTF). Figure 2 shows the MTFs for both collimators. These curves confirm the expected increase in image degradation that occurs when the distance between object and collimator increases and when the object is imaged inside a scattering medium. These results, in essence, support the findings shown in Fig. 1.

At the lower spatial frequencies, the larger number of scattered photons causes a sharp peak in the MTF curves. This effect is more pronounced for the low-energy collimator, especially when imaging is done with scattering medium present.

For the higher spatial frequencies, there is a sharper decline in the MTF values for the medium-energy collimator. This effect persists when the two collimators are compared for similar imaging geometries (distance, presence or absence of scattering medium). The point at which the low-energy collimator retains a greater content of the higher spatial frequencies is shown in Table 1.

Using the line source images obtained on Day 7, the MTFs ascribable to I-124 show a large component at only the lowest spatial frequencies (Fig. 3). Compared with the previous curves, the small-amplitude, high-frequency components of the MTFs are partly explained by a higher content of random noise.

Relative sensitivity. Table 2 shows the total proportion of measured counts due to the I-124 contaminant (4.1%). As expected, under similar geometries the number of detected events due to I-124 is greater for the low-energy collimator. Similarly, the number of counts accepted is greater when more scattered photons are produced, due either to the medium surrounding the line source

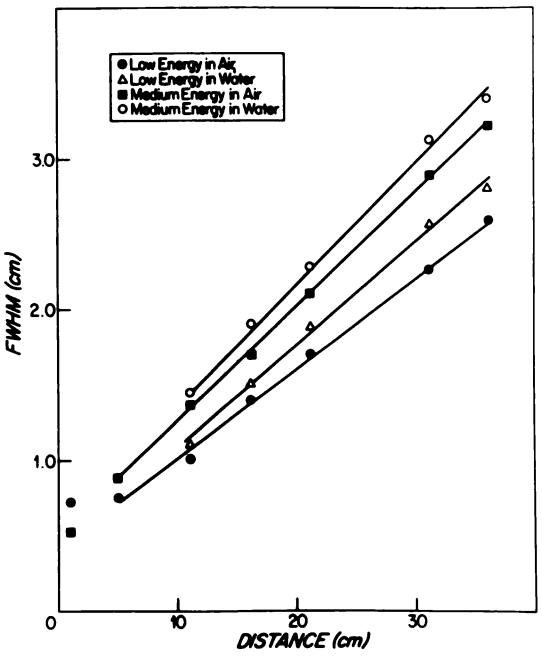

FIG. 1. Two-dimensional FWHM values plotted against distance from collimator face. Even when imaging line sources centered in water-filled cylinder, 20 cm in diam, general-purpose collimator consistently out-performs medium-energy collimator.

TABLE 1. LIMITS OF SPATIAL FREQUENCY FOR INCREASED INFORMATION CONTENT USING LOW-ENERGY COLLIMATOR

	Frequency* (cycle/pixel)	Frequency* (cycle/cm)	Amplitude†
Air, 11 cm	0.09	0.38	0.34
Air, 21 cm	0.04	0.19	0.54
Water, 11 cm	0.09	0.37	0.20
Water, 21 cm	0.05	0.21	0.28

* Frequency at which MTF value of low-energy collimator becomes larger than that of the medium-energy.

† Amplitude of the MTF at that frequency.

TABLE 2. % CONTRIBUTION OF I-124 TO THE TOTAL COUNTS (4.1% OF TOTAL MIXTURE)

	Air 11 cm	Air 21 cm	Water 11 cm	Water 21 cm
Low-energy collimator	26.1%	17.5%	36.1%	28.0%
medium-energy collimator	11.2%	7.1%	14.6%	12.0%

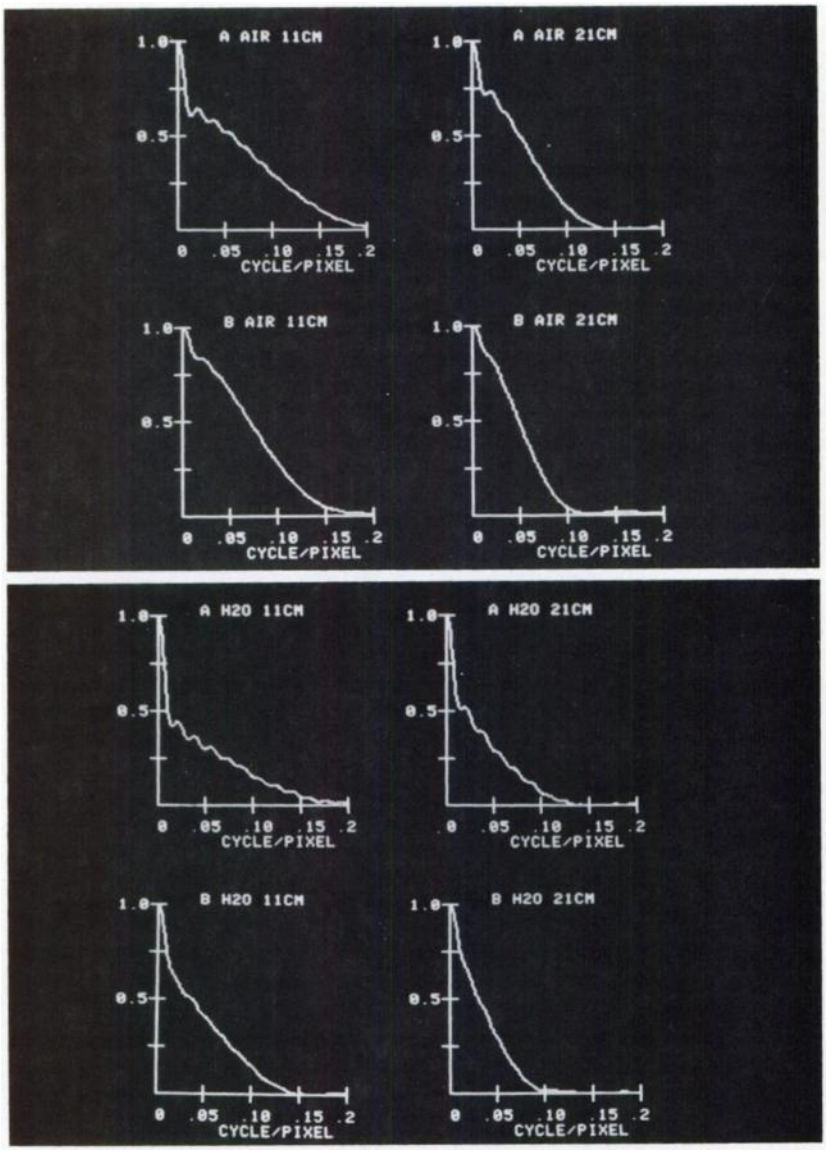

FIG. 2. Modulation transfer functions for low-energy general-purpose (A) and medium-energy (B) collimators, determined from line sources imaged in air (upper four) or at center of (20 cm diam) water-filled cylinder (lower four). One pixel corresponds to 0.237 cm. General-purpose MTF values extend further into high spatial frequencies despite prominent low-frequency content due to scatter from I-124.

or to collimator proximity. These measurements reflect an almost constant density of background counts in the acquired images.

A more direct comparison of collimator sensitivity to I-123 reveals that, with respect to the medium-energy collimator, the low-energy collimator is less sensitive when images are acquired in air: by 4.5% at 11 cm and 7.2% at 21 cm. This loss is more severe for images taken through water: 14.6% at 11 cm and 15.6% at 21 cm (Table 3). This last observation probably reflects the greater sensitivity of the medium-energy collimator to photons scattered through small angles.

Tomographic images. Figure 4 shows transaxial slices through a cylindrical phantom for both collimators. The cylindrical targets, with the 30:1 in the center, were set in a background activity of 0.3 μCi/cc. Blurring of the high-contrast target edges is marked with the medium-energy collimator.

DISCUSSION

When imaging of radionuclides emitting higher photon energies (due either to the decay scheme or to inseparable contaminant isotopes) is attempted, the performance of collimators can be expected to suffer significant degradation (*1*,*2*,*6*). At least two physical processes will affect collimator performance: (a) the amount of septal penetration by the higher-energy photons and their subsequent release of energy in the imaging window due to partial deposition of energy in the crystal and (b) the amount of scattered photons generated in the object being imaged.

We evaluated the effect of the higher-energy photons (511-1691 keV) from I-124 on the image quality for an Anger camera equipped with both low-energy general-purpose and medium-energy collimators. Other authors have pointed out that the high-energy photons of pure I-123 also lead to some loss in spatial resolution and image quality (*6*). We opted not to measure these effects separately but to measure overall collimator response to I-123 contaminated with I-124, since, in the final evaluation, we are interested in the use of this isotopic mixture for clinical imaging.

Our results show that the resolution of the low-energy collimator is better than that of the medium-energy (Fig. 1). This holds whether scattering milieu is present or not. These measurements are, in effect, worst-case estimates of the general-purpose collimator's FWHM, since no attempt was made to correct for the image background generated by the high-energy photons. As was

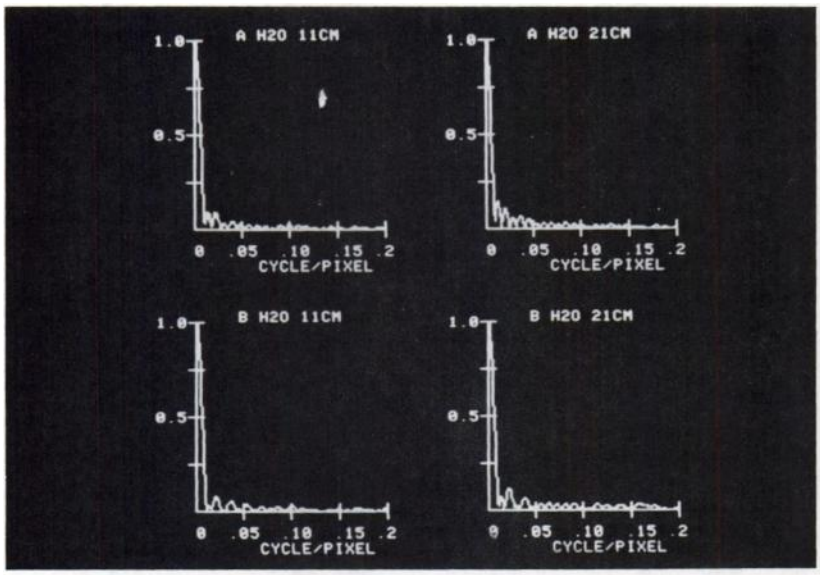

FIG. 3. Modulation transfer functions of line sources imaged on Day 7 (159-keV window) show large amplitude mostly in lower spatial frequencies. Fluctuations in higher frequencies are due principally to poor statistics and to some spatial aliasing.

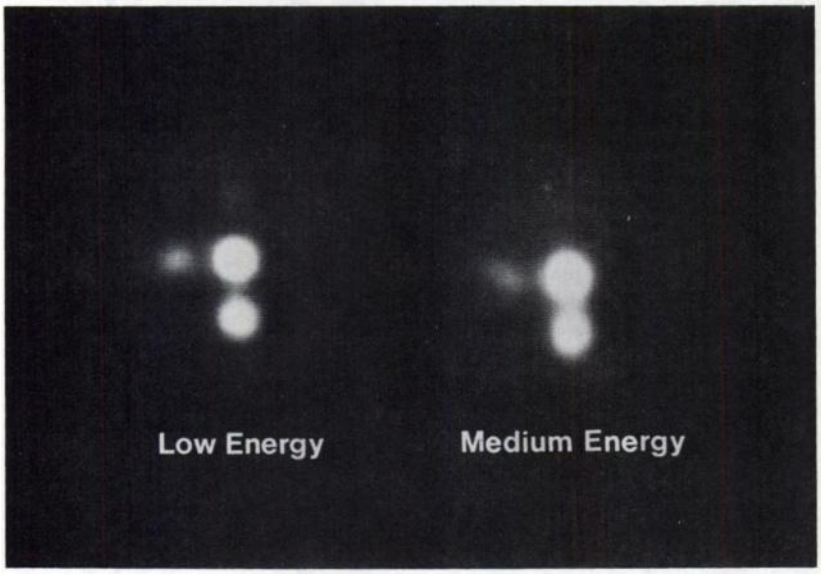

FIG. 4. Transaxial slices obtained after tomographic reconstructions of cylindrical phantom. High contrast targets (30:1, 15:1, 6:1, 3:1) are clearly seen in both cases. There is some blurring at edges in those reconstructions of data acquired with medium-energy collimator.

shown by these experiments, these photons add an almost constant (low spatial frequencies) number of counts to the planar images. Such favorable performance characteristics may be due, in part, to the large collimator thickness (41 mm).

System resolution, per se, does not permit one to predict the quality and contrast fidelity of acquired images. For this reason, collimator performance was assessed with the aid of calculated MTFs. Such an approach permits one to evaluate collimator performance at higher spatial frequencies and, thus, to predict which one will result in a more accurate transfer of information (*5*).

Our calculated MTF is markedly modified by the presence of high-energy photons of I-124. This effect is more clearly seen at the lower spatial frequencies and is more prominent with the general-purpose collimator (the MTF abruptly falls with increasing spatial frequencies). Septal penetration by the primary photons, and by a larger number of photons issuing from scattering events in the water-filled phantom, is the most likely source of this phenomenon.

For similar imaging geometries (i.e., distance from collimator, presence or absence of a scattering milieu) the medium-energy collimator's MTFs are larger than those of the general-purpose collimator (Fig. 2). There is, however, a cross-over point where the general-purpose collimator retains high spatial frequency components (Table 1). This improvement in image quality for two-dimensional imaging is also seen after tomographic reconstruction.

In the case of the high-contrast phantom, the targets are more

TABLE 3. SENSITIVITY OF LOW-ENERGY COLLIMATOR RELATIVE TO THAT OF MEDIUM-ENERGY COLLIMATOR

	Air 11 cm	Air 21 cm	Water 11 cm	Water 21 cm
To total counts acquired (4.1% I-124)	1.15	1.04	1.14	1.03
to 100% I-124	2.68	2.58	2.83	2.42
to 100% I-123	0.955	0.928	0.854	0.844

sharply circumscribed on the reconstructed slices obtained with the general-purpose collimator (Fig. 4). This collimator would therefore have a distinct advantage in any quantification scheme requiring an edge-detection algorithm to delineate volume contours.

When dealing with statistically limited images, collimator sensitivity is of primary importance. The overall sensitivity of the general-purpose collimator to the I-123/I-124 mixture is greater than that of the medium-energy collimator (Table 3). When the contribution from I-124—a quantity known not to add significantly to overall image quality (Fig. 3)—is eliminated, the sensitivity of the general-purpose collimator is, at worst, 85% of that of the medium-energy collimator (Table 3). This small disadvantage is amply offset by the improved transfer response offered by the general-purpose collimator, since increased sensitivity per se cannot overcome the true limitation in fidelity transfer between object and image experienced by the medium-energy collimator.

In conclusion, our results favor the use of a low-energy general-purpose collimator during tomographic imaging with tracers labeled with I-123 contaminated with I-124. The increase in image quality and resolution offsets the amount of image degradation caused by the high-energy I-124 photons. Our results apply especially to collimators with a large enough thickness (in our case 41 mm) to prevent significant photon penetration.

ACKNOWLEDGMENTS

The authors thank Mrs. Margaret J. R. Senechal for her assistance in preparing this manuscript, and Richard LePage for his technical assistance in preparing sufficiently concentrated solutions of the I-123/I-124 mixture.

REFERENCES

1. McKeighen RE, Muehllehner G, Moyer RA: Gamma camera collimator considerations for imaging ^{123}I. *J Nucl Med* 15:328-331, 1974
2. Graham LS, Poe ND, Robinson GD: Collimation for imaging the myocardium. II. *J Nucl Med* 17:719-723, 1976
3. Zielinski FW, MacDonald NS, Robinson GD: Production by compact cyclotron of radiochemically pure iodine-123 as iodide for synthesis of radiodiagnostic agents. *J Nucl Med* 18:67-69, 1977
4. Holman BL, Hill TC, Magistretti PL: Brain imaging with emission computed tomography and radiolabeled amines. *Invest Radiol* 17:206-215, 1982
5. Beck RN, Zimmer LT, Charleston DB, Harper PV, Hoffer PB: Advances in fundamental aspects of imaging systems and techniques. In *IAEA Symposium on Medical Radioisotope Scintigraphy*. Monte Carlo, Monaco, 1972, pp 3-45
6. Bolmsjö MS, Persson BRR, Strand S-E: Imaging ^{123}I with a scintillation camera. A study of detection performance and quality factor concepts. *Phys Med Biol* 22:266-277, 1977